ANALYSIS OF THE MEDIUM FIELD Q-SLOPE IN SUPERCONDUCTING CAVITIES MADE OF BULK NIOBIUM

G. Ciovati#, Thomas Jefferson National Accelerator Facility (TJNAF), Newport News, VA, USA
J. Halbritter, Forschungszentrum Karlsruhe, Karlsruhe 76021, Germany

Abstract

The quality factor of superconducting radio-frequency cavities made of high purity, bulk niobium decreases with rf field in the medium field range (peak surface magnetic field between 20 and about 100 mT). The causes for this effect are not clear yet. The dependence of the surface resistance on the peak surface magnetic field is typically linear and quadratic. This contribution will present an analysis of the medium field *Q*-slope data measured on cavities at different frequencies treated with buffered chemical polishing (BCP) at Jefferson Lab, as function of different treatments such as post-purification and low-temperature baking. The data have been compared with a model involving a combination of heating and of hysteresis losses due to "strong-links" formed on the niobium surface during oxidation.

INTRODUCTION

Superconducting radio-frequency (rf) cavities made of bulk niobium are commonly used in particle accelerators for a wide variety of applications. The quality factor of a cavity, $Q_0 = \omega U/P = G/R_s$, is defined as the ratio between the cavity stored energy (U) and the power dissipated in the cavity walls in one rf radian (P/ω). An equivalent definition is the ratio of the geometry factor G, given by cavity shape and rf mode, and the surface resistance R_s of the wall material. A typical plot of the cavity quality factor as a function of the peak surface magnetic field, B_p, in the TM_{010} mode in the range 20–100 mT often shows a more or less marked degradation, referred to as "medium field *Q*-slope" [1, 2]. Understanding the origin of the medium field *Q*-slope is important in order to develop a cavity treatment which minimizes it, allowing to produce cavities with reduced cryogenic losses and enhanced rf breakdown fields. In this paper we will present an analysis of the medium field *Q*-slope data of Nb cavities with a resistance ratio of RRR > 200, which did undergo different treatments such as low-temperature "in-situ" baking and post-purification and with different crystallographic properties, such as polycrystalline niobium with different average grain sizes and single crystal. The surface treatment before high-power rf test in superfluid helium is a standard one used for niobium cavities and consists of buffered chemical polishing (BCP) with a mixture of HNO_3, HF and H_3PO_4 in ratio 1:1:1, removing approximately 20 μm of niobium from the inner cavity surface*, followed by an high pressure rinse (HPR) with ultra-pure water to eliminate surface contaminations, especially dust particles.

MODELS FOR THE MEDIUM FIELD Q-SLOPE

One of the causes for the increase of the surface resistance at increasing rf field is the thermal impedance between the inner cavity surface, where the heat is generated, and the helium bath, cooling the outer cavity surface. Halbritter [3] introduced the following ansatz for R_s as a function of B_p:

$$R_s(T,B_p) = R_{s0}(T)\left[1+\gamma^*(T)\left(\frac{B_p}{B_c}\right)^2 + O\left(B_p^4\right)\right], \qquad (1)$$

where R_{s0} is the surface resistance at about 20 mT being the sum of the BCS surface resistance, $R_{BCS0}(T)$, and the residual resistance, R^0_{res}. B_c = 200 mT is the thermodynamic critical field at $T = 0$ of niobium [4] and T is the He bath temperature. The medium field *Q*-slope is represented by the parameter $\gamma^*(T)$ which depends on $R_{BCS0}(T)$, Kapitza resistance, R_K, thermal conductivity, κ, and wall thickness, d. Recently, Gurevich [5] estimated the increase of the BCS surface resistance due to the pair-breaking effect caused by a high rf field and added an additional term to $\gamma^*(T)$, inversely proportional to T^2.

Our experimental results often show a linear increase R_s vs. B_p, in addition. A possible cause for such dependence is the presence of hysteresis losses due to Josephson fluxons (JF) at "strong-links", as described by Halbritter in Ref. [6]. Such "strong-links" are oxide-filled boundaries caused by oxidation of fresh Nb surfaces or by enforced oxidation of already existing grain boundaries. The critical current density J_{cJ} of these "strong-links" is of the order of $10^9 - 10^{11}$ A/m^2, much higher than that of "weak-links" in high-T_c superconductors but still smaller than the critical depairing current density $J_{cp} \simeq 4\times10^{12}$A/m². Halbritter gives the following expression for the hysteresis losses, R_{hys}:

$$R_{hys}(B_p) \approx \frac{4}{3\pi}\frac{\omega}{2J_{cJ}\left[1+(\omega/\omega_0)^2\right]^{3/2}}\frac{2\lambda}{a_J}B_c\left(\frac{B_p}{B_c}\right) = R^1_{res}\left(\frac{B_p}{B_c}\right), \qquad (2)$$

where a_J is the island size and ω_0 is a characteristic fluxon nucleation frequency. ω_0 decreases from about 5 GHz for $J_{cJ} \simeq 10^{10}$A/m² ("fast" Josephson fluxons) to about 10 MHz for $J_{cJ} \simeq 10^{12}$A/m² ("slow" Abrikosov fluxons) [6]. The dependence given by Eq. (2) has been observed for 1.5 GHz Nb thin films cavities with R^1_{res} between 100-1000 nΩ [7]. R_{hys} is predicted to be temperature independent for $T < T_c/2$.

* After initial removal of ≈ 100 μm.

gciovati@jlab.org

ANALYSIS OF EXPERIMENTAL RESULTS

Since both, quadratic and linear dependencies, of R_s vs. B_p were measured the experimental data have been fitted by the following expression for the field and temperature dependence of the surface resistance:

$$R_s\left(T,B_p\right)=R_{s0}\left(T\right)+R^1_{res}\left(T\right)\left(\frac{B_p}{B_c}\right)+R_{s0}\left(T\right)\gamma^*\left(T\right)\left(\frac{B_p}{B_c}\right)^2. \quad (3)$$

The fitting parameters are R_{s0}, γ^* and R^1_{res} and are subjected to the constraint of being greater than zero. Table 1 shows the values of the fitting parameters and of the fit correlation factor r^2 obtained from a comparison with R_s vs. B_p data measured on a polycrystalline Nb single cell cavity, resonating at 1.467 GHz in the TM_{010} mode, published in Ref. [8] in detail. The cavity was post-purified by heat treatment at 1400°C for 4 h in a vacuum furnace. The values shown in Table 1 are averaged over seven consecutive rf tests after this post-purification, separated by 10 µm BCP, before and after a low-temperature "in-situ" baking at temperatures between 70 and 180°C for 48 h. The values in Table 1 show a stronger quadratic dependence at T below 2 K and an increase by about a factor of two of R^1_{res} by baking. Data taken at 2.2 K, above the superfluid transition temperature of liquid He, show a dominant quadratic dependence with γ^* values above about fifteen [8]. Figure 1 shows the increase of the surface resistance, $R_s - R_{s0}$, as a function of B_p/B_c before and after baking at 105°C for 48 h.

Table 1: Average values of fit parameters to Eq. (3) and correlation factor r^2 obtained from a comparison with R_s vs. B_p data at 2 K and 1.37 K, before and after baking at different temperatures in the range 70 – 180°C for 48 h. Data were taken on a niobium single cell cavity resonating at 1.467 GHz in the TM_{010} mode which was previously post-purified. The temperature-independent residual resistance, R^0_{res}, increased from 5.3 ± 0.1 nΩ before baking to 6.3 ± 0.1 nΩ after baking.

	T = 2 K	
	Before baking	After baking
R_{s0} (nΩ)	21.6 ± 0.1	15.2 ± 0.2
R^1_{res} (nΩ)	11.6 ± 1.1	20.2 ± 1.9
γ^*	0.04 ± 0.10	0.10 ± 0.24
r^2	0.952	0.950
	T = 1.37 K	
	Before baking	After baking
R_{s0} (nΩ)	4.81 ± 0.03	4.82 ± 0.06
R^1_{res} (nΩ)	2.27 ± 0.31	4.39 ± 0.47
γ^*	1.36 ± 0.14	1.46 ± 0.17
r^2	0.982	0.988

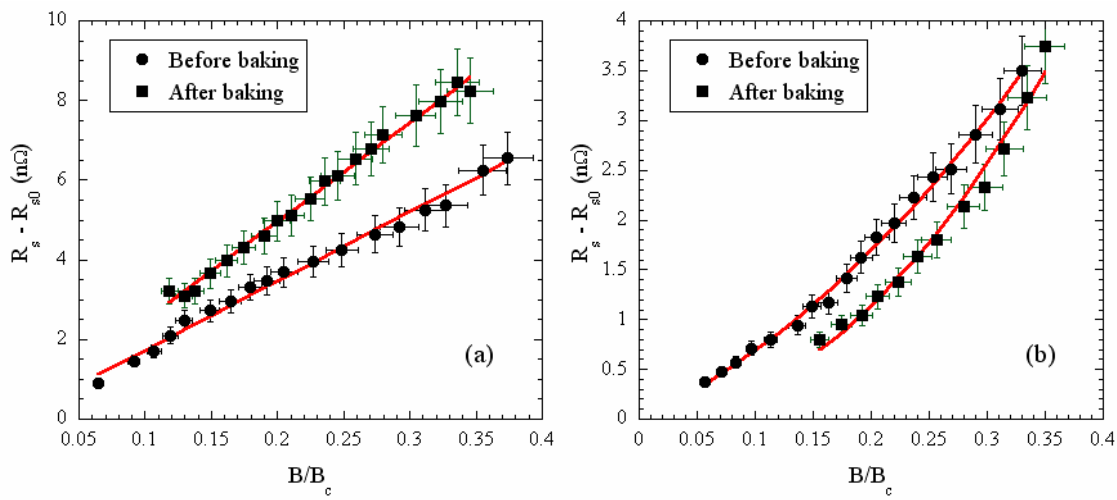

Figure 1: Increase of the surface resistance as a function of B_p/B_c before and after baking at 105°C for 48 h measured at 2 K (a) and 1.37 K (b) for a single cell cavity which was post-purified. Solid lines represent fits with Eq. (3).

Table 2 shows the average values of R^1_{res}, γ^*, R_{s0} and r^2 obtained from fits using Eq. (3) with data on the TM_{010} (1.466 GHz) and on the TE_{011} (2.819 GHz) mode in a polycrystalline Nb single cell cavity published in Ref. [9] in detail. Before post-purification the quadratic term is the main component as medium field Q-slope for both modes, while directly after post-purification the linear term dominates. Baking significantly enhances R^0_{res} and R^1_{res}. The values of the fit parameters for the TM_{010} mode after post-purification are consistent with the ones showed in Table 1 on a different cavity. The increase of R^0_{res} by post-purification was mainly due to an increase of the trapped residual Earth's magnetic field due to a drift of the current in the compensation coils. Figure 2 shows $R_s - R_{s0}$ as a function of B_p/B_c before and after post-purification for the TM_{010} and TE_{011} modes.

Table 2: Average values of the fit parameters R^1_{res}, γ^* and R_{s0} and correlation factor r^2 for both, TM_{010} (1.466 GHz) and TE_{011} (2.819 GHz) modes, at 2 K before and after baking, before and after post-purification treatment on a niobium single cell cavity. The average values of the temperature-independent residual resistance and is also indicated.

	Before post-purification			
	Before baking		After 100-120 °C baking	
	TM_{010}	TE_{011}	TM_{010}	TE_{011}
R^0_{res} (nΩ)	5.6 ± 0.6	10.1 ± 0.9	9.0 ± 0.5	12.3 ± 0.9
R_{s0} (nΩ)	26.9 ± 0.2	51.5 ± 0.4	16.7 ± 0.2	36.3 ± 0.2
R^1_{res} (nΩ)	7.46 ± 1.46	0.003 ± 3.7	27.1 ± 1.3	5.32 ± 2.40
γ^*	1.55 ± 0.11	2.76 ± 0.14	0.97 ± 0.13	3.34 ± 0.14
r^2	0.995	0.994	0.998	0.997
	After post-purification			
	Before baking		After 100-120 °C baking	
	TM_{010}	TE_{011}	TM_{010}	TE_{011}
R^0_{res} (nΩ)	8.5 ± 0.6	12.0 ± 1.2	17.0 ± 0.2	14.8 ± 0.7
R_{s0} (nΩ)	28.7 ± 0.1	79.3 ± 0.3	23.3 ± 0.3	52.7 ± 0.3
R^1_{res} (nΩ)	16.4 ± 1.1	24.1 ± 2.8	34.1 ± 2.0	71.9 ± 1.5
γ^*	0.01 ± 0.07	0.00 ± 0.06	0.00 ± 0.13	0.25 ± 0.03
r^2	0.987	0.988	0.993	0.989

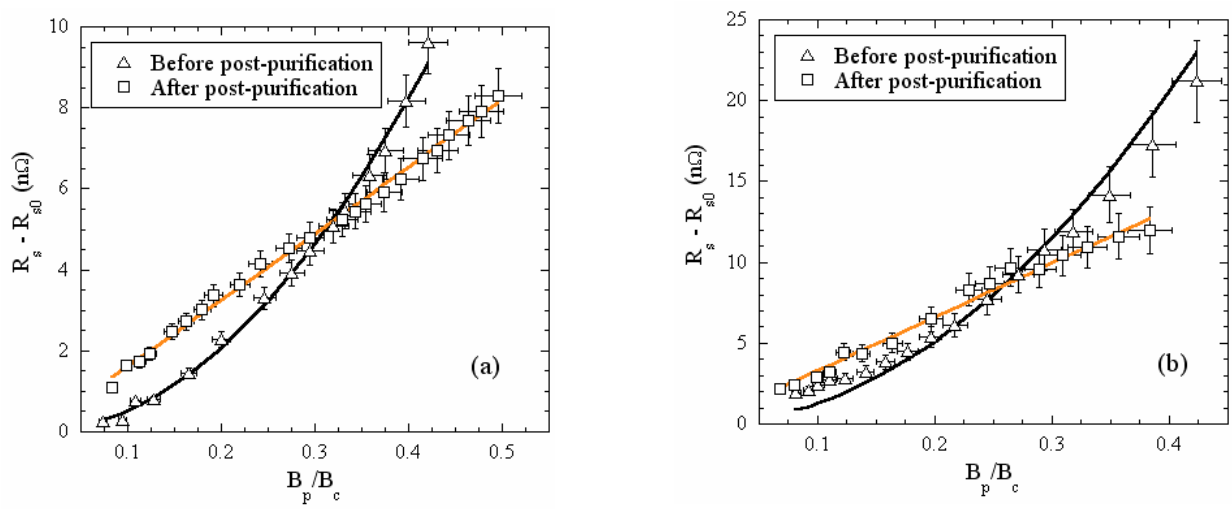

Figure 2: Increase of the surface resistance as a function of B_p/B_c before and after post-purification measured at 2 K in the TM_{010} (a) and TE_{011} (b) modes of a single cell cavity. Solid lines represent fits with Eq. (3).

Table 3 shows the values of the fit parameters and the fit correlation factor obtained from a comparison with data measured on a single cell cavity made of single crystal niobium, resonating at 2.256 GHz in the TM_{010} mode [10]. The cavity had been post-purified at 1250°C for about 12 h. The values in Table 3 indicate that, before baking at 120°C for 48 h, the dependence of R_s vs. B_p is linear and becoming enhanced by baking. Plots of $R_s - R_{s0}$ as a function of B_p/B_c for the single crystal cavity measured at different temperatures, before and after baking, are shown in Fig.3, indicating at low B_p a similar linear slope between 1.55 and 2 K before baking where at higher fields the $R_s(B_p)$–growth slows down.

Table 3: Fit coefficients and correlation factor of Eq. (3) for data on a post-purified 2.256 GHz single crystal niobium cavity taken at different temperatures before and after baking at 120°C for 48 h. The value of the temperature-independent residual resistance, R^0_{res}, is 0.8 ± 0.4 nΩ before baking and 10.0 ± 0.3 nΩ after baking.

Single crystal cavity, before bake				
T (K)	R_{s0} (nΩ)	R^1_{res} (nΩ)	γ^*	r^2
2	29.1 ± 0.2	12.3 ± 1.3	0.00 ± 0.06	0.983
1.84	18.3 ± 0.2	14.3 ± 1.1	0.00 ± 0.08	0.994
1.69	8.7 ± 0.2	11.8 ± 1.0	0.95 ± 0.14	0.997
1.55	4.2 ± 0.1	20.0 ± 0.6	0.00 ± 0.2	0.999
Single crystal cavity, after bake				
T (K)	R_{s0} (nΩ)	R^1_{res} (nΩ)	γ^*	r^2
2	24.3 ± 1.1	55.4 ± 2.1	1.03 ± 0.05	0.980
1.84	15.0 ± 1.0	43.5 ± 1.5	1.77 ± 0.13	0.978
1.69	11.8 ± 0.2	36.7 ± 0.6	2.52 ± 0.08	0.995
1.55	10.1 ± 0.2	24.5 ± 0.8	2.81 ± 0.07	0.975

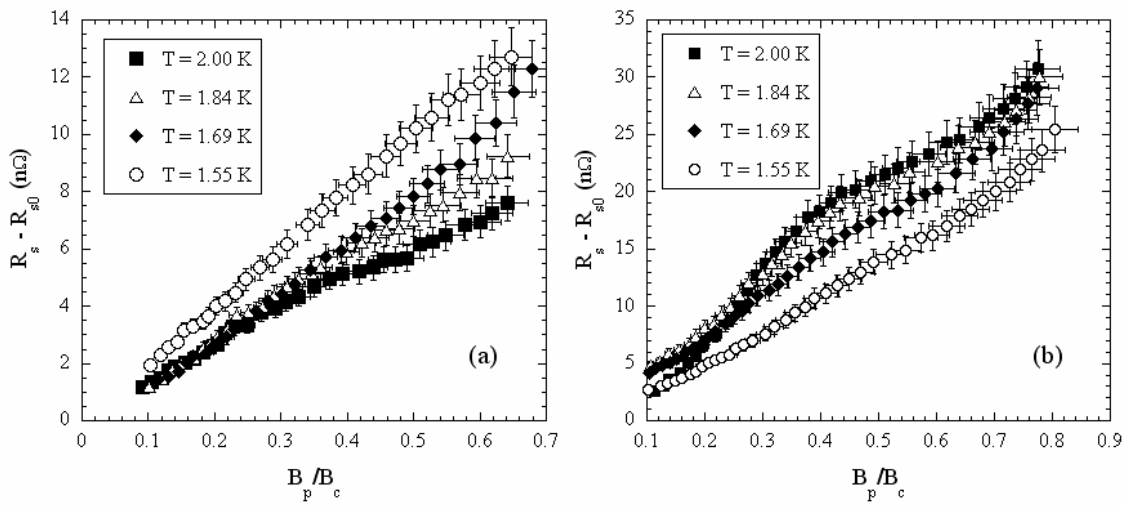

Figure 3: Increase of the surface resistance as a function of B_p/B_c before (a) and after baking (b) at 120°C for 48 h measured at several temperatures on a single cell made of single crystal niobium after post-purification.

DISCUSSION

In this section we estimate the value of the parameters of Eq. (2) and (3) in comparison with the data in Tables 1-3. We model the single crystal data of Table 3 first and we add then oxidized grain boundaries to model the data of Tables 1-2. $R^0_{res} < 1$ nΩ at 2.2GHz, qualitatively hints a large J_{cJ} ($> 10^{11}$A/m^2) due to oxidation of fresh, RRR > 200 Nb single crystal surfaces. One can speculate that such oxidation before baking may show $a_J \simeq 100$ nm, $J_{cJ} \simeq 8\times10^{11}$A/m² and $\omega_0 \simeq 0.06$ GHz yielding the R^1_{res}-values summarized in Table 4a. Subsequent baking yields further oxidation, decreasing J_{cJ} towards $J_{cJ} \simeq 6\times10^{11}$A/m and $\omega_0 \simeq 0.09$ GHz describing Table 3 well.

To model the data of Tables 1-2, we consider oxidized grain boundaries with an average grain size of $a_J \simeq$ 100μm before and ≃ 2 mm after crystal growth during post purification at temperatures greater than 1200°C for several hours. In Table 4b we assume critical current

density values lower than for oxidized single crystal: $J_{cJ} \simeq 8\times10^{10}$A/m² with $\omega_0 \simeq 0.5$ GHz and 4×10^{10} A/m^2 with $\omega_0 \simeq 5$ GHz before and after post-purification, respectively. Crystallites growth without O (NbO) evaporation by post-purification at 1200°C reduces the density of extended grain boundaries where the O tends to segregate, yielding a lower J_{cJ}, as proposed by Halbritter [6] to explain the increase of the linear slope coefficient for niobium films with increasing grain size. The values of R^1_{res} predict the correct order of magnitude of the fit results of Table 2. The changed ω-dependence of R^1_{res} from $\propto 1/\omega^2$ to $\propto \omega$ given by Eq. (2) is due to the J_{cJ} decrease by baking yielding a change of ω_0 modeled well in Table 4b.

To model the quadratic slope coefficients γ^* before and after post-purification, at frequencies 1.467 GHz and 2.819 GHz, in Table 4b we use Equation (8a) of Ref. [3]. γ is the sum of γ^* and an additional pair-breaking term, given in Ref. [5]. Thermal conductivity and Kapitza resistance values for polycrystalline Nb were obtained from Refs. [11-13] for wall thickness of 2.8 mm. The thermal conductivity of the single crystal Nb was obtained from Ref. [14]. The values of Table 2 at 2 K are roughly consistent with theoretical estimate of γ^* in Table 4b, while the pair-breaking contribution (γ) seems to be too large. In addition, γ^* is predicted to be reduced below 2 K due to the exponentially decreasing BCS losses, but such dependence was not observed. Even the addition of the pair-breaking effect as proposed by Gurevich [5] does not explain the higher value of γ^* below 2 K. It is also interesting to notice the slow temperature dependence of the product $R_{s0}\gamma^*$ in Table 3, increasing from 25 nΩ to 28 nΩ between 2 and 1.55 K. The estimated value of the quadratic slope coefficient is reduced by post-purification, due to the increased thermal conductivity of the niobium.

Table 4a: Theoretical estimate of the linear coefficient R^1_{res} and of the quadratic term γ^* of Table 3 with parameters J_{cJ}, ω_0 and a_J described in Section 4 for strong-links due to oxidation of a single crystal Nb surface before and after baking. The niobium thermal conductivity and Kapitza resistance are supposed to be unchanged by the low-temperature baking.

	Before baking	After baking
$R_{res}{}^1$ (nΩ)	11.3	50.8
γ^*(2 K)	0.26	0.26
γ(2 K)	1.92	1.92

Table 4b: Theoretical estimate of the linear ($R_{res}{}^1$) and quadratic (γ* and γ) coefficients at 1.467 and 2.819 GHz before baking, before and after post-purification of polycrystalline niobium.

	Before post-purification		After post-purification	
	1.467 GHz	2.819 GHz	1.467 GHz	2.819 GHz
$R_{res}{}^1$ (nΩ)	131	40	35	50
γ^*(2 K)	0.67	1.47	0.19	0.78
γ^*(1.37 K)	0.12	0.42	0.06	0.26
γ(2 K)	2.33	3.40	1.72	2.59
γ(1.37 K)	0.80	2.17	0.74	2.01

CONCLUSION

The analysis of the increase of the surface resistance as a function of the peak surface magnetic field ($B_p \simeq 20$ – 100 mT, so called "medium field Q-slope") on rf cavities made of bulk niobium shows the presence of both linear and quadratic terms. The linear term has been interpreted as due to hysteresis losses by "strong-links" created at Nb surfaces by oxidation. The quadratic term is due to overheating of the cavity inner surface due to the thermal impedance of the niobium and of the niobium/helium interface.

A cavity made of single crystal niobium exhibits a marked linear dependence of R_s vs. B_p and a strong temperature dependence of the slope coefficient which is altered by the low-temperature baking. These effects cannot be completely explained by our simplified model and require further investigation. The observed increase of R^1_{res} by baking and post-purification can be described by a reduction of J_{cJ}.

An increase of the quadratic one was obtained from the analysis of the data on polycrystalline cavities below 2 K, possibly suggesting locally enhanced losses [6, 15]. In addition, recent results on temperature maps of the outer cavity surface as a function of B_p [16] show that localized defects contribute to the medium field Q-slope, confirming localized heating as suggested in Ref. [3, 6].

This work was supported by the U.S. DOE Contract No DE-AC05-84ER40150 Modification No. M175, under which the Southeastern Universities Research Association (SURA) operates the Thomas Jefferson National Accelerator Facility.

REFERENCES

[1] G. Ciovati, Proceeding Pushing the Limits of RF Supercond. Workshop, Argonne IL (Ed. K.-J. Kim, ANL-05/10, 2005), p. 52.
[2] B. Visentin, see Ref. [1], p. 94.
[3] J. Halbritter, Proceeding 38th Eloisatron Workshop, Erice, 1999 (Eds. L. Cifarelli and L. Maritato, World Scientific, Singapore, 2001), p. 9 and Proceeding. 10th Workshop on RF Supercond., Tsukuba, Japan, 2001 (Ed. S. Noguchi, KEK, 2003), p.292.
[4] R. A. French, Cryogenics 8 (1968) 301.
[5] A. Gurevich, see Ref. [1], p. 17.
[6] J. Halbritter, J. Appl. Phys. 97 (2005) 083904.
[7] M. A. Peck, Ph.D. Dissertation (Technical University Wien, Austria, 1999).
[8] G. Ciovati, J. Appl. Phys. 96 (2004) 1591.
[9] G. Ciovati and P. Kneisel, see Ref. [1], p. 74.
[10] P. Kneisel, G. Ciovati, G. Myneni, T. Carneiro and J. Sekutowicz, Proceeding of the 2005 Particle Accelerator Conf., Knoxville TN, 2005, (Ed. N. Holtkamp), TPPT076.
[11] P. Bauer, G. Ciovati, G. Eremeev, A. Gurevich, L. Lilje, N. Solyak and B. Visentin, this conference, TuP01.
[12] J. Amrit, C. Z. Antoine, M. X. Francois, and H. Safa, Cryogenics 47 (2002) 499.
[13] S. Bousson, M. Fouaidy, T. Junquera, N. Hammoudi, J. C. Le Scornet and J. Lesrel, Proceeding 8th Workshop on RF Supercond., Santa Fe NM, 1999 (Ed. F. Krawczyk, LANL, 2000), p. 263.
[14] G. R. Myneni, this conference, MoP08.
[15] J. Halbritter, this conference, SuA05, and unpublished.
[16] G. Ciovati, Ph.D. Thesis, Old Dominion University, Norfolk, 2005.